

Myeong Hee Moon<sup>1</sup>  
 Hyun-Joo Kim<sup>1</sup>  
 Se-Jin Lee<sup>2</sup>  
 Yoon-Seok Chang<sup>2</sup>

## Pinched inlet gravitational split-flow thin fractionation of airborne particles and analysis of size dependent level of PCDD/Fs

<sup>1</sup>Department of Chemistry, Yonsei University, Seoul, Korea

<sup>2</sup>School of Environmental Science & Engineering, Pohang University of Science & Technology, Pohang, Korea

Fine particles in air have a direct influence on human health because they carry toxic chemicals that can be deposited in the human lung when inhaled. Thus, particle size distribution and size dependent level of contamination of the airborne particles are important parameters for the study and assessment of environmental pollution. In this study, gravitational split-flow thin (SPLITT) fractionation (or GSF), a semi-preparative scale separation technique for particles, was applied for the continuous size sorting of airborne particles collected in urban area. About 2.0 g of airborne particles was fractionated into four different size intervals (<1.5, 1.5–2.5, 2.5–5.0, and >5.0  $\mu\text{m}$ ), and the collected fractions were examined by electron microscopy for particle size distribution and analyzed for the size dependent levels of polychlorinated dibenzo-*p*-dioxins and furans (PCDD/Fs). It was found that more than 60% of particles including dissolved matters in weight were smaller than 5.0  $\mu\text{m}$  and they contained more than 86% of the total PCDD/Fs amount in airborne particles.

**Key Words:** SPLITT; Pinched inlet GSF; Airborne particles; Size characterization; PCDD/Fs; Size dependent distribution of dioxin

Received: January 24, 2005; revised: March 2, 2005; accepted: March 5, 2005

DOI 10.1002/jssc.200500040

### 1 Introduction

Particulate matter (PM) in the atmosphere is one of the major concerns in air pollution since these particles carry a mixture of potentially toxic chemicals such as polychlorinated dibenzo-*p*-dioxins and furans (PCDD/Fs), polycyclic aromatic hydrocarbons (PAHs), heavy metals, *etc.* [1–4]. Among the toxic materials, PCDD/Fs originate mostly from various combustion processes and possibly from forest fires and volcanoes [5, 6]. Atmospheric particles are a complex mixture of primary and secondary particles, organic and inorganic compounds from a variety of natural and anthropogenic sources. Primary particles are found both as the coarse fraction that is primarily from the earth and predominantly the fine fraction which is mainly composed of soluble inorganic species, organic compounds, and heavy metals that are products of anthropogenic production processes [1, 4]. Especially fine particles with diameter smaller than 2.5  $\mu\text{m}$  (PM<sub>2.5</sub>) are the greatest health concern since, when inhaled, they can be deposited and accumulate in the lungs where they can cause respiratory disease [7, 8]. Therefore, particle size distribution in the atmosphere plays a critical role in air quality as well as in the control of residence time and the removal mechanism of atmospheric particles. In addition, it is an

important factor affecting human health since fine particles provide a larger surface area to adsorb insoluble organic pollutants than coarse particles do. Moreover, these fine particles in the atmosphere are washed out by rain, transported, and finally accumulate on the surface of aquatic sediments. Contamination of the sediments results in the bioaccumulation of toxic materials in marine biota and eventually in humans through the food chain [9–12]. Thus, it is very important to determine the particle size of ambient particles and the size-dependent level of contamination because the study of the size-distribution pattern of airborne particles can provide information about their origin.

Many studies have been conducted on the distribution of PAHs, PCDD/Fs, and metals with respect to the size of airborne particles [2, 3, 7, 10]. Mostly, these were based on the size fractions obtained by a cascade impactor during the collection of airborne particles. The cascade impactor is widely used for multistage size fractionation and for the collection of airborne particles from a large amount of air. In this study, split-flow thin fractionation (SPLITT fractionation or SF) [13–18], a relatively new kind of continuous and rapid separation technique, is utilized for the accurate fractionation of fine airborne particles. Recently, gravitational SPLITT fractionation (GSF) has been effectively applied on a semi-preparative scale for size sorting of environmental particles such as fly ash from a municipal solid waste incinerator (MSWI) and mar-

**Correspondence:** Prof. Myeong Hee Moon, Department of Chemistry, Yonsei University, Seoul, 120–749, Korea  
 Phone: +82 2 2123 5634. Fax: +82 2 364 7050.  
 E-mail: mhmoon@yonsei.ac.kr.

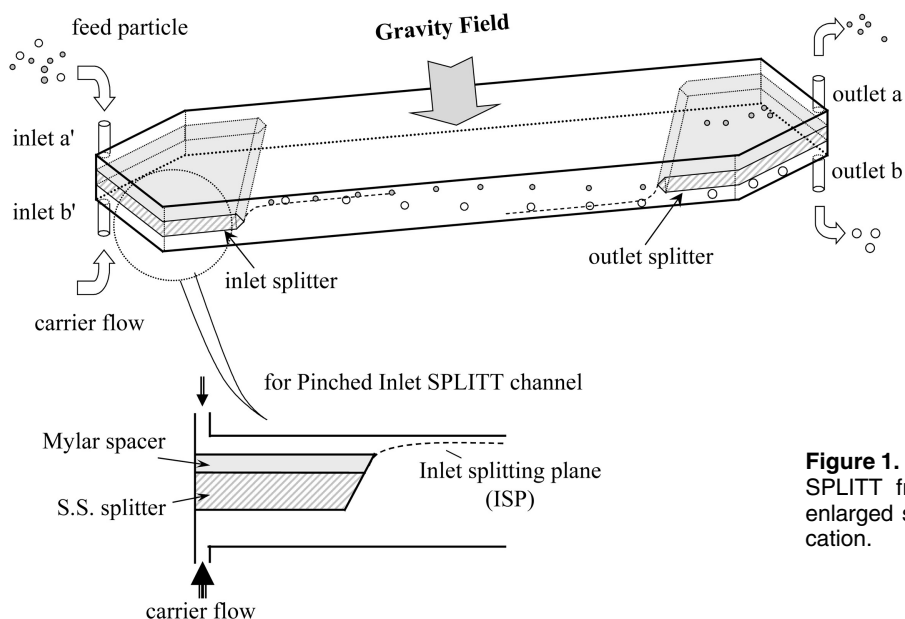


**Figure 1.** Schematic illustration of gravitational SPLITT fractionation (GSF) channel with an enlarged side view of the pinched inlet modification.

ine sediments [17, 19–21]. The resulting size fractions were examined to study size-dependent levels of PCDD/Fs and their homologue patterns using high resolution gas chromatography/high resolution mass spectrometry (HRGC/HRMS), and to examine heavy metals related to particle sizes using inductively coupled plasma-atomic emission spectrometry (ICP-AES).

GSF is carried out in a thin, empty rectangular channel equipped with two splitters on both channel inlet and outlet as shown in **Fig. 1**. In GSF, particles are continuously introduced at channel inlet-*a'* in suspended form while a relatively high speed carrier stream enters through the carrier inlet-*b'*. Due to the compression effect of the carrier stream (usually set to be faster than the sample feed rate), particles leaving the inlet splitter are immediately pushed toward the upper wall of the channel, and begin their migration toward the end of the channel. While migrating along the GSF channel, particles settle across the flow stream by gravity. Therefore, particles that settle slowly will emerge from the upper outlet-*a*, whereas the faster ones exit from the lower outlet-*b*. Eventually, fractions collected from both outlets contain particles larger or smaller than a certain diameter (or cut-off diameter) that is readily adjusted by regulating the flow rates of the two outlets. The cut-off diameter,  $d_c$ , in a GSF channel can be readily calculated from the following relationship [13]

$$d_c = \sqrt{\frac{18\eta(\dot{V}(a) - 0.5\dot{V}(a'))}{bLG(\rho_p - \rho)}} \quad (1)$$

where  $\eta$  is the viscosity of carrier fluid,  $b$  the channel breadth,  $L$  the channel length,  $G$  the gravity,  $\rho_p$  the particle density,  $\rho$  the density of carrier fluid,  $\dot{V}(a')$  the feed flow rate, and  $\dot{V}(a)$  the carrier flow rates.

In this study, the GSF technique was used for the fractionation of airborne particles collected in a city area with heavy traffic flow. A pinched inlet GSF (PI-GSF) channel [20–22], a GSF channel modified to improve separation efficiency by reducing the thickness of the sample inlet path as shown in the enlarged view of Fig. 1, was used for fractionating airborne particles at three different cut-off diameters ( $d_c = 5.0, 2.5,$  and  $1.5 \mu\text{m}$ ). The total four different size fractions ( $<1.5, 1.5\text{--}2.5, 2.5\text{--}5.0,$  and  $>5.0 \mu\text{m}$ ) were examined by electron microscopy for particle size distribution and by HRGC/HRMS for the total PCDD/Fs concentration according to the sizes.

## 2 Experimental

### 2.1 PI-GSF

A PI-GSF channel built in house was used for this study. The channel structure was the same as reported in the literature [20–22]. A single channel dimension ( $8 \times 23 \text{ cm}$  in breadth  $\times$  length) was used throughout the fractionation process. The thickness of the channel was 50, 100, and  $300 \mu\text{m}$  for the pinched inlet, carrier inlet, and total channel, respectively. The splitter was made from  $100 \mu\text{m}$  thick stainless steel plate. While two Mylar spacers ( $50 \mu\text{m}$  each) were layered above the splitter, the beginning end region of one spacer right above the inlet splitter was left without cut, and the top Mylar spacer was cut through so that sample can be introduced. Underneath the splitter, a  $100\text{-}\mu\text{m}$  thick Mylar spacer was used, so that the total channel thickness becomes  $300 \mu\text{m}$  in the open channel region (details can be found in ref. [20]).

The airborne particles examined in this study were collected starting from October, 2004 for approximately 4

**Table 1.** Experimental flow rate conditions of PI-GSF for airborne particle sample.

$d_c$ [ $\mu\text{m}$ ]	Fraction No.	Volumetric flow rate [mL/min]	
		$\dot{V}(a')$	$\dot{V}(b')$
5.0	1b	1.0	4.8
		0.5	4.5
2.5	2b	0.5	1.4
		0.3	1.3
1.5	3a, 3b	0.2	0.5
		0.1	0.4

For all cases,  $\dot{V}(a') = \dot{V}(b)$  and  $\dot{V}(b') = \dot{V}(a)$ . The same channel dimension ( $8 \times 23$  cm: breadth  $\times$  length) was used for all runs.

months on the roof of the college of science building at Yonsei University by using a high volume Model HV-1000s air sampler from Sibata Scientific Technology Ltd., (Tokyo, Japan). Particles were collected on glass fiber filters that were baked at  $450^\circ\text{C}$  for 12 h before sampling and were equilibrated for 24 h in a desiccator with silica gel before weighing. Each collection took 48 h at a flow rate of 700 L/min and the total sampling volume was approximately  $5.1 \times 10^4$  m<sup>3</sup>. Sample filters from a series of collections were put into a beaker with 2 L of the GSF carrier solution, and were sonicated to isolate the attached particles. The carrier solution was prepared with ultrapure water ( $>18$  M $\Omega$ ) containing 0.1% FL70, a mixture of ionic and nonionic surfactant, and 0.02% NaN<sub>3</sub> as a bactericide. Crude particles were dried at  $105^\circ\text{C}$  and weighed. The density measured was 1.28 g/cm<sup>3</sup>. For GSF, 2.0 g of airborne particles were dispersed in the carrier solution at a concentration of 0.5% (w/v). For each fractionation step, a two stage fractionation process was applied: a rough cut at a moderate feed rate and a precision cut at a low feed rate by re-injecting the collected particles. Flow rate conditions are listed in **Table 1**.

For feeding airborne particles to inlet- $a'$ , a Minipulse 3 peristaltic pump from Gilson (Villiers-le-Bel, France) was used. The carrier liquid was pumped through the inlet- $b'$  by using an FMI lab pump from Fluid Metering Inc. (Oyster, NY, USA). Eluted particles were concentrated on-line using a PCUU (particle concentrator with upstream ultrafiltration) and the filtrate was circulated to be re-used for carrier solution as explained in earlier reports. For on-line filtration of eluted particles in a PCUU, a membrane having a pore size of 1.0  $\mu\text{m}$  was used. Details of the PCUU can be found in earlier work [17]. For the control of flow rates at both outlets, a fine metering valve from Crawford Fitting Co. (Solon, OH) was used at the upper outlet of PCUU. Particle sizes were measured from electron micrographs taken by JSM-5610L Scanning Electron Microscope from Jeol (Tokyo, Japan).

## 2.2 PCDD/Fs analysis

For sample preparation prior to the analysis of PCDD/Fs in airborne particles, US EPA method 1613 was used. Each airborne particle fraction collected from PI-GSF was dried and spiked with 1 ng of internal standards, a mixture of <sup>13</sup>C<sub>12</sub>-labeled PCDD/F, from Wellington Laboratory (Ontario, Canada), then was extracted for 16 h using toluene under glass Soxhlet thimbles. Each extract was washed with sulfuric acid until colorless and then with distilled water that was saturated with hexane for neutralization. Sample purification was carried out with a multilayer silica column as described in an earlier publication [20]. Finally, all the samples were concentrated with N<sub>2</sub> gas and 1 ng of <sup>13</sup>C<sub>12</sub>-labeled PCDD/F recovery standard mixture was added. Separation and characterization of PCDD/Fs were performed with a model 6890 HRGC (using a DB-5MS column, 60m  $\times$  0.25mm-ID  $\times$  0.25  $\mu\text{m}$  film thickness) from Hewlett-Packard (Palo Alto, CA, USA) interfaced with a model 700T HRMS from Jeol (Tokyo, Japan). The temperature gradient was as follows: an initial temperature of  $140^\circ\text{C}$  for 4 min, a linear ramp of 15 K/min to an isothermal hold of  $220^\circ\text{C}$  for 3 min, another ramp of 1.5 K/min to an isothermal hold of  $240^\circ\text{C}$  for 3 min, and a final ramp of 4 K/min to an isothermal hold of  $310^\circ\text{C}$  for 6 min. For HRMS analysis, a SIM (single ion monitoring) method was employed under positive EI conditions set at 38 eV with a resolution over 10 000. Selection of PCDD/Fs peaks was made for those having isotope ratios within 15% of theoretical values and having a signal-to-noise ratio larger than 2.5 simultaneously. The recovery range of <sup>13</sup>C<sub>12</sub>-labeled PCDD/F internal standards was 50–120%, meeting protocols of EPA method 1613.

## 3 Results and discussion

Fractionation of airborne particles in the PI-GSF channel was carried out in the decreasing order of cut-off diameters; 5.0, 2.5, and 1.5  $\mu\text{m}$ . Since most airborne particles collected in this study were found to be smaller than 10  $\mu\text{m}$ , an initial fractionation was made to cut them at  $d_c = 5.0$   $\mu\text{m}$  at a feed rate,  $\dot{V}(a')$ , of 1.0 mL/min. and a carrier flow rate,  $\dot{V}(b')$ , of 4.8 mL/min based on Eq. (1). The particle fraction eluted at channel outlet- $b$  is expected to be larger than 5.0  $\mu\text{m}$  while the fraction at outlet- $a$  is smaller than 5.0  $\mu\text{m}$ . In order to improve separation efficiency in PI-GSF, a two-stage fractionation process was utilized: an initial fractionation was carried out at a relatively fast feed rate to increase throughput and the collected fraction was subjected to PI-GSF at a slow feed rate for fine control of cut-off diameter. Feeding at a reduced feed rate will lower the throughput; however, it was found to improve the accuracy of separation [19, 20]. After an initial fractionation of airborne particles, the fraction collected at the

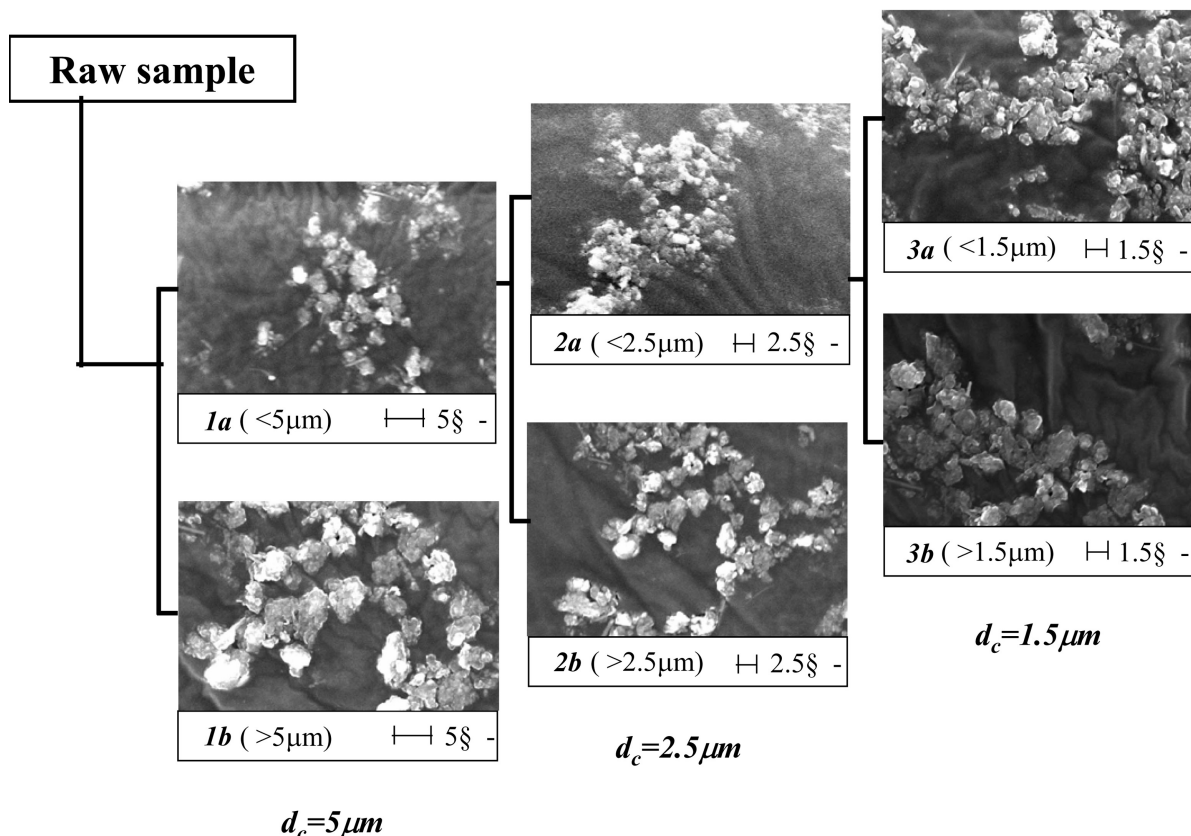


**Figure 2.** Electron micrographs of airborne particle fractions collected from three sequential runs using PI-GSF. Flow rate conditions are explained in the text. Each cut-off diameter and microscopic scales are marked inside the figure.

outlet-*b* was concentrated and this was re-injected into the PI-GSF channel to remove any smaller particle at a reduced feed rate (= 0.5 mL/min.). The flow rate condition for the precision run was slightly modified as shown in Table 1 but it generated the same cutoff diameter. The particle fraction collected at the upper outlet of a precision cut was mixed with the previous fraction that was smaller than 5.0 μm and that collected at the lower outlet was stored for a secondary analysis. The particle fractions were named after the designation of the outlet port with numbers representing the fractionation step at different cut-off diameter, such as fraction-1*a* and fraction-1*b*. **Figure 2** shows the electron micrographs of collected fractions through the entire PI-GSF runs. In the micrographs, most particles in the fraction-1*a* appeared to be smaller than 5.0 μm. Since airborne particles were not flat in shape, the shape factor was not expected to affect the elution of particles significantly. Thus, it was unlikely that oversized particles would be observed in the fraction expected to contain particles smaller than  $d_c$ . However, in the fraction-1*b* that was supposed to contain particles larger than the cut-off diameter, few undersized particles appeared in the micrograph. If the density of airborne particles was not homogeneous, it can be expected that

some heavy particles will be co-eluted with the fraction-1*b* due to the large sedimentation coefficient. By counting the number of particles larger than 5.0 μm, the percentage value for fraction-1*b* was found to be 85.5%, as listed in **Table 2**. For the measurement, about 150 to 200 particles were counted for each fraction. While approximately 15% of particles are smaller than the cut-off diameter, this percentage recovery value is similar to the effectiveness observed in earlier studies dealing with sediments [19, 21].

Particles collected in fraction-1*a* were further fractionated at a cut-off diameter of 2.5 μm while fraction-1*b* was put aside for PCDD/Fs analysis. The same 2-stage fractionation process was applied by changing the flow rate conditions according to the decreased cut-off diameter as listed in Table 1. Collected particles were examined as electron micrographs and particle size was measured. The particle size distribution of each fraction was plotted in **Fig. 3**, which was based on particle counting at a small diameter interval. Fraction-1*b* and fraction-2*b* show that few undersized particles (smaller than each corresponding cut-off diameter) are found to elute together. Fraction-3*b* shows few particles outside of the size interval (1.5–2.5 μm); however the number percentage value for the fraction-3*b*

**Table 2.** The number percentage values and measured weight of particles contained in each fraction obtained by PI-GSF, and the total PCDD/Fs concentration values for particles in each fraction measured by HRGC/HRMS expressed with per unit mass of particles and unit volume of air for each fraction. Total air volume is 50918.1 m<sup>3</sup>.

	Expected diameter range [μm]	Number percentage [%]		Weight [g]	Number average diameter ±std. dev [μm]	Total PCDD/Fs [ng/g]	Total PCDD/Fs [pg/m <sup>3</sup> ] <sup>a)</sup> in air
		> <i>d<sub>c</sub></i>	<i>d<sub>c</sub></i>				
fraction-1 <i>b</i>	>5.0	85.5	14.5	0.730	6.3 ± 1.3	5.02	0.072
fraction-2 <i>b</i>	2.5–5.0	78.7	21.3	0.133	3.0 ± 0.7	76.6	0.200
fraction-3 <i>b</i>	1.5–2.5	84.2	15.8	0.090	1.8 ± 0.3	67.9	0.120
fraction-3 <i>a</i>	<1.5	8.8	91.2	0.142	1.0 ± 0.3	69.2	0.193
residue				0.060		37.3	0.044
GSF solution				0.845 <sup>b)</sup>		0.84	0.257

<sup>a)</sup> Total PCDD/Fs amount rescaled into in pg per unit volume of air.

<sup>b)</sup> Weight of matter presumed as dissolved in GSF carrier solution.

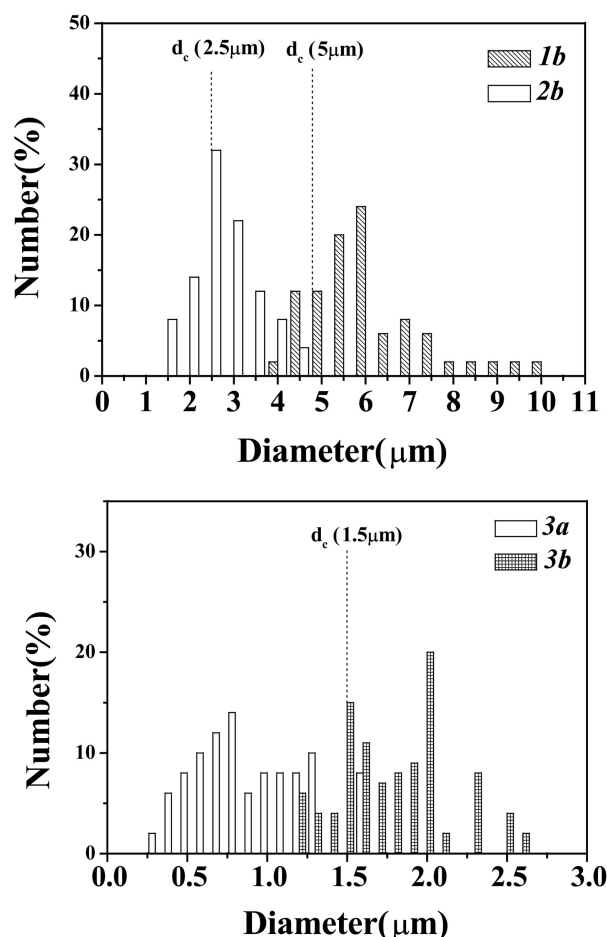


**Figure 3.** Size distributions of collected particles at each fraction by microscopic measurement. About 150–200 particles were measured for each fraction.

(84.2%) is not markedly poor. Fraction-3*a* was found to contain 91.2% of particles in number smaller than 1.5 μm. Number average particle diameters of each fraction

measured from electron micrographs are listed in Table 2 and they showed good agreement with the size range of each fraction expected from theory. From these results, fractionation of airborne particles using PI-GSF was successfully accomplished without deviating significantly from theoretical expectations. All collected fractions were concentrated and dried to measure their weights and the results are listed in Table 2. While particles larger than 5.0 μm were a major size group in terms of weight distribution, fractions of smaller particles were not. The value of the residue in Table 2 represented the weight measured for particles that were entangled with filter debris (caused by sonication to remove particles from glass fiber filter) and left within the PI-GSF channel without undergoing migration. In addition, it was found that a considerable amount of particles seemed to be dissolved in the carrier solution during the PI-GSF run. There is a possibility of losing particles in tubing and connections. After all fractionation work, the carrier solution was circulated by a tangential filtration method using a flat rectangular channel built for this process. The special channel built for tangential filtration had a sheet membrane (a pore size of 10 kDa) placed inside instead of a splitter in SPLITT channel system, and the filtrate was collected while the retentate was circulated to be concentrated. However, it was found that more than 40% of the particles by weight (0.845 g calculated from the total 2.00 g of particles employed) were dissolved in the carrier solution without being retrieved. These were thought to dissociate into ultrafine particles or considered to be soluble salts. Particles in the retentate were further concentrated by using down stream filtration and they were added to the fraction-3*a*.

In Table 2, calculated results of PCDD/Fs concentration for each fraction and for the carrier solution are listed. They were expressed in two different units; one with ng/g of particles and the other with pg/m<sup>3</sup> considering the volume of air (50918.1 m<sup>3</sup>) collected. It shows that the total

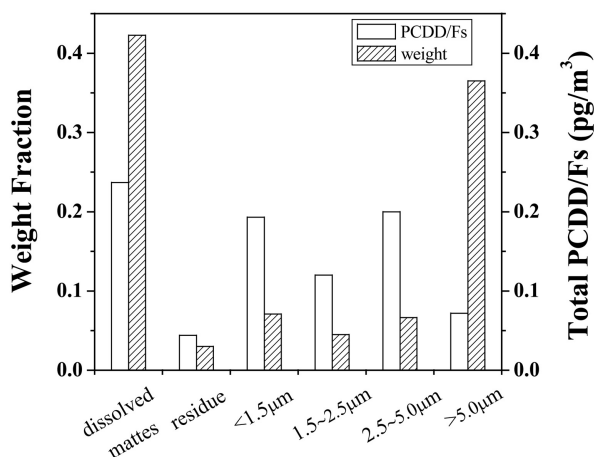


**Figure 4.** Relative weight distribution and the fraction of total PCDD/Fs for GSF fractions of airborne particles.

concentration of PCDD/Fs for particle fraction larger than 5.0  $\mu\text{m}$  is much smaller than those of the smaller fractions. However, the weight of the fraction-1b was 5–7 times larger than those of the others, and therefore the total PCDD/Fs concentration in air was not very low for particles larger than 5.0  $\mu\text{m}$ . It was found that a particle size range of 2.5–5.0  $\mu\text{m}$  exhibited the highest PCDD/Fs concentration and smaller fractions appeared to contain a similar level of PCDD/Fs. This was similar to the results obtained from fly ash and sediment particles reported earlier due to the increase of surface area for small particles. In earlier reports, carrier solutions used for SPLITT fractionation of fly ash particles or sediments did not show a detectable amount of PCDD/Fs due to the very low solubility of PCDD/Fs in water. However, the concentration value expressed for the carrier solution in Table 2 was not negligible, even though the carrier solution after PI-GSF runs was filtered by the tangential flow filtration method. It can be deduced that soluble matter or ultrafine particles possibly dissolved in carrier solution contributed to the detection of PCDD/Fs. The amount of total PCDD/Fs per gram of the carrier solution ( $\approx 0.84$  ng/g) was very small compared to those of the other particle fractions. This supports the idea that matter in the filtrate could be mostly soluble components in air. Normalized weight distributions of airborne particles are plotted together with the total concentration of PCDD/Fs in Fig. 4. It is clearly shown that the concentration values of total PCDD/Fs contained in particles smaller than 5.0  $\mu\text{m}$  are high (more than 48% in total) though the total weight of the three fractions is relatively small.

### 3 Conclusions

This study demonstrated the use of GSF for the continuous separation of airborne particles into four different size

groups and showed that the collected particles can be further analyzed for the size-dependent level of PCDD/Fs. Since particle separation in GSF is based on differences in settling coefficient of particles under gravity in flowing streams, particle separation can be accurately controlled by adjusting the flow rates based on the theory. It was found from the experiments that more than 60% of particles by weight including dissolved matter were smaller than 5.0  $\mu\text{m}$  and they contained more than 86% of the total PCDD/Fs amount in air. This indicated that the total PCDD/Fs amounts in airborne particles are closely associated with fine particles smaller than 5.0  $\mu\text{m}$ .

### Acknowledgments

This study was supported by the KOSEF (Korea Science & Engineering Foundation) Fund 1999-2-124-001-5.

### References

- [1] T.F. Beddeman, *Environ. Sci. Technol.* **1988**, *22*, 361–367.
- [2] J.E. Oh, Y.S. Chang, E.-J. Kim, D.-W. Lee, *Atmos. Environ.* **2002**, *36*, 5109–5117.
- [3] F.F. Alvarez, M.T. Rodriguez, A.J.F. Espinosa, A.G. Daban, *Anal. Chim. Acta* **2004**, *524*, 33–40.
- [4] T. Ohura, T. Amagai, T. Sugiyama, M. Fusaya, H. Matsushita, *Atmos. Environ.* **2004**, *38*, 2045–2054.
- [5] R.E. Alcock, K.C. Jones, *Environ. Sci. Technol.* **1996**, *30*, 3133–3143.
- [6] J.A. Prange, C. Gaus, R.E. Weber, O. Papke, J.F. Muller, *Environ. Sci. Technol.* **2003**, *37*, 4325–4329.
- [7] S.S. Park, Y.J. Kim, *Atmos. Environ.* **2004**, *38*, 1459–1471.
- [8] C.A. Pope III, M.J. Thun, N.M. Namboodiri, D.W. Dockery, J.S. Evans, F.E. Speizer, C.W. Heath, *Amer. J. Resp. Critical Care Med.* **1993**, *151*, 669–674.
- [9] W.R. Sherman, R.E. Keenan, D.G. Gunster, *J. Toxicol. Environ. Health* **1992**, *37*, 177–195.
- [10] J.D. Abbott, S.W. Hinton, *Environ. Toxicol. Chem.* **1996**, *15*, 1163–1165.
- [11] E.A. Mamontova, A.A. Mamontov, E.N. Tarasova, *Organohalogen Comp.* **2001**, *52*, 247–250.
- [12] T. Sakurai, J.-K. Kim, N. Suzuki, J. Nakanishi, *Chemosphere* **1996**, *10*, 2007–2020.
- [13] J.C. Giddings, *Sep. Sci. Technol.* **1985**, *20*, 749–768.
- [14] Y. Jiang, A. Kummerow, M. Hansen, *J. Microcol. Sep.* **1997**, *9*, 261–273.
- [15] C. Contado, F. Riello, G. Blo, F. Dondi, *J. Chromatogr. A.* **1999**, *845*, 303–316.
- [16] C.B. Fuh, *Anal. Chem.* **2000**, *72*, 266A–271A.
- [17] M.H. Moon, D. J. Kang, D.W. Lee, Y.S. Chang, *Anal. Chem.* **2001**, *73*, 693–697.
- [18] C. Contado, F. Dondi, *J. Sep. Sci.* **2003**, *26*, 351–262.
- [19] M.H. Moon, H.J. Kim, S.-Y. Kwon, S.-J. Lee, Y.-S. Chang, H. Lim, *Anal. Chem.* **2004**, *76*, 3236–3243.
- [20] M.H. Moon, D.J. Kang, H. Lim, J.-E. Oh, Y.-S. Chang, *Environ. Sci. Technol.* **2002**, *36*, 4416–4423.
- [21] M.H. Moon, H.-J. Kim, Y.-O. Jung, S.-J. Lee, Y.-S. Chang, *J. Sep. Sci.* **2005**, in press.
- [22] M.H. Moon, D.J. Kang, S.-Y. Kwon, S. Lee, *J. Sep. Sci.* **2003**, *26*, 1675–1682.